Regenerative Engineering and Translational Medicine
https://doi.org/10.1007/s40883-019-00145-y

3D-Printed Bioreactor Enhances Potential for Tendon Tissue Engineering

Brittany L. Banik[1] · Justin L. Brown[1]

Received: 10 July 2018 / Revised: 12 December 2019 / Accepted: 24 December 2019

Abstract

Bioreactors have immense value within tissue engineering by enabling important control over design inputs within a microenvironment; however, they are often complex and expensive. Herein, we demonstrate a strategy where a bioreactor was 3D-printed as a means to provide an accessible route to culture scaffolds under physiological inputs and to determine an ideal tendon scaffold structure based on remodeling and degradation events. Furthermore, real-time monitoring of tissue remodeling is introduced through the bioreactor design. Following in vitro uniaxial stretch conditioning, scaffolds were positively altered to reflect improved biomechanical function, enhanced extracellular matrix (ECM) content, and increased mechanical properties of elastic moduli. A bioreactor was constructed to meet the following criteria: real-time readout of resistance, ability to be easily cleaned and sterilized, control of strain, speed, and time parameters, and capability to withstand 3 weeks of continuous load with minimal maintenance. The scaffolds cultured in a dynamic setting showed improved mechanics and promising ECM and collagen content generated. Overall, the bioreactor was effective as a tool to provide mechanical culture conditions that promote the tendon cell niche. The bioreactor supports the scaffolds as a possible therapeutic venture in tendon tissue engineering. Additionally, the 3D-printed bioreactor is a significant contribution to the tissue engineering field by making dynamic culturing more accessible for researchers.

Lay Summary

Bioreactors present physiological and dynamic conditions for tissue testing and are crucial in tissue engineering for product development, standardization, quality control, and large-scale synthesis. The low-cost, 3D-printed, programmable bioreactor provides cyclic stretch to scaffolds with real-time resistance readout and demonstrates tissue changes over time. The bioreactor enhances scaffold biomechanics and biofunctionality towards natural tendon by promoting cell alignment through mechanical force. The design components are culture chamber for tendon constructs, motor control of uniaxial stretching, and a base for stabilization. The results from conditioning scaffolds in the bioreactor lend to a better understanding of how specific inputs affect tissue outcomes.

Keywords Cyclic strain bioreactor · Tendon · Tissue engineering · 3D printing

Introduction

Bioreactors are devices that provide numerous benefits to tissue engineering applications. These mechanical devices permit control over critical inputs such as temperature, pH, gas concentration, humidity, pressure, and mechanical forces; allow for tissue growth before transplantation; function as a tool to expand cells; assist in organ support; and serve as dynamic environments for mixing nutrients and reducing gradient formations of toxins. Despite the apparent benefits, current cyclic bioreactors are expensive, difficult to tailor towards experimental use, and often require researchers to rely on another

Description of Future Works Future works to expand this project include the following: integrating a Graphic User Interface (GUI) for the bioreactor to simplify programming, testing silk as a scaffold material, and consideration to overall scaffold design that would incorporate the enthesis.

Electronic supplementary material The online version of this article (https://doi.org/10.1007/s40883-019-00145-y) contains supplementary material, which is available to authorized users.

✉ Justin L. Brown
jlbbio@engr.psu.edu

[1] Department of Biomedical Engineering, The Pennsylvania State University, 122 CBE Building, University Park, PA 16802, USA

Published online: 21 January 2020

group for testing, which makes bioreactors challenging to acquire and incorporate into experimentation.

Tendons are mechanosensitive, connective tissues that join muscles to bones. These musculoskeletal tissues are critical for daily activities—joint stability, locomotion, and transmitting forces. Because of the wear-and-tear tendons seen over time and the broad of those affected by damaged tendons, there is an inherent need for a better tendon replacement. Despite the need for tendon regeneration options, a sufficient synthetic structure that provides a directive environment to enhance cell matrix secretion and supports an appropriate structure for cell orientation does not exist. Bioreactors have been used in the tendon tissue engineering field as a way to enhance scaffold biomechanics and biofunctionality towards natural tendon. More specifically, the application of mechanical force promotes specified cell alignment and response during culture.

Advancements have been made in the design of effective bioreactor systems for biomimetic soft tissue [1]. Youngstrom et al. describe a custom bioreactor that utilizes the Flexcell's™ Uniflex™ cyclic strain system with a LabVIEW program for operation; the bioreactor consists of modular vessels that hold one scaffold at a time [2, 3]. The experimental results based on decellularized equine tendon seeded with bone marrow-derived mesenchymal stem cells suggest that a cyclic linear strain of 3% at 0.33 Hz for 60 min per day promoted tendon differentiation compared to the other experimental groups of 0%, 5%, and an adult tendon removed from sport horses (control). Another group, Wang et al., developed a bioreactor system with components constructed from AISI 316 stainless steel (culture chamber, tissue clamps, hooks), 6063 aluminum (frame), and glass (cover). The bioreactor functioned based on a step motor and programmable logic control and was used to apply cyclic tensile strains of 3%, 6%, and 9% with 0.25 Hz, 8 h per day, for 6 days. Based on the frequency and applied loading time for the group's experiments, 6% strain was determined to be the ideal strain to maintain structural integrity and cellular function for tendons [4, 5].

Bioreactor-type systems have also been designed to better understand tenocyte mechanobiology with specific interest in tenocyte mechanotransduction. Maeda et al. created a device to analyze the effects of oscillatory fluid shear stress and cyclic tensile strains separate and in combination with tenocytes on intracellular Ca^{2+} concentration. The collagen fiber alignment and tenocyte organization were mimicked through microgrooves in a flow unit [6].

Bioreactors provide dynamic environments to aid in in vitro tissue growth and development by utilizing mechanical methods to influence necessary biological cues and physical regulatory signals [7, 8]. Systems capable of applying a strain or increasing intracellular contractility directly affect biochemical signaling in cells through mechanotransduction [9]. This mechanotransduction can occur through a number of force sensitive proteins either linking the cell to the ECM or linking the cell to adjacent cells. The bioreactor approach discussed primarily affects the cell/ECM interaction through modulating focal adhesion signaling [9–11]. The application of a strain on the scaffold results in reinforcement of focal adhesions and the cytoskeleton as the cell responds to the applied strain [10, 12–14]. Furthermore, focal adhesion signaling directly affects GTPase activation, which has potential in regulating the differentiation of stem cells towards tendon lineages [14–20]. Bioreactors output more viable, effective, and reliable tissues at a larger-scale production level because cell stretching encourages tissue anabolism and cell-mediated ECM restoration [1]. In this project, a low-cost, programmable bioreactor with real-time resistance readout was created to demonstrate tissue response towards tendon relative to culturing in the bioreactor. The presented 3D-printed, cost-effective bioreactor synthesis allows for flexibility in design changes as well as construction ease. As a 3D-printed device, the part files can be accessible worldwide.

Materials and Methods

Bioreactor Components The bioreactor components were created in Solidworks and saved as STL (STereoLithography) files (see Supplementary Information). A FormLabs desktop Form 1+ 3D printer was utilized to print the small bioreactor parts by stereolithography (SLA), which is based on layer-by-layer photopolymerization. Because of the need to ensure the media vessel would not leak or breed contamination, the container was not 3D-printed; instead, a Plexiglas cup was utilized. Due to the larger surface area and increased printing time, the bioreactor base was outsourced to Stratasys Direct Manufacturing and printed via selective laser sintering (SLS) with Nylon 12 material. The mechanics were driven by a Haydon Kerk linear actuator (Haydon Kerk 43HP-2.33.815, 43000 Series, size 17), stepper motor controller and drive, and programmable drive package (IDEA™ Stepper Motor Controller and Drive, Haydon Kerk PCM4826E). The Haydon-Kerk linear actuator step angle was 1.8°, which is equal to a resolution of 200 steps per resolution. A conductive rubber cord stretch sensor comprised of carbon black impregnated rubber (Adafruit, Product ID: 519) was utilized as a real-time resistance readout to monitor scaffold remodeling. As the sensor cord stretched, the resistance increased. Likewise, at a relaxed state, the cord returns to the original resistance output. A simple method was used to cover the bioreactor system—a Rubbermaid Tupperware container was turned upside down with the bioreactor base resting on the lid of the container and the clear Tupperware bottom turned upside down over the bioreactor to prevent outward contamination. An Extech EX330 Autoranging Mini Multimeter was attached to the

conductive resistance cord through alligator clips to obtain resistance information.

Bioreactor Construction

The three main components of the presented bioreactor design are: (1) tissue culture chamber that houses six tendon constructs, (2) motor control of the uniaxial stretching mechanism through an easy-to-use programming utility, and (3) a main base to stabilize the entire device. The bioreactor was modeled in Solidworks with attention given to reduce the overall bioreactor footprint and printing cost. A heated, UV-cure system was incorporated into manufacturing the final bioreactor parts. Pieces were removed from the printer base, repeatedly dipped for 2 min in isopropyl alcohol, and soaked in isopropyl alcohol for 10 min to remove the residual stickiness leftover from the resin. To finalize the polymerization and reach optimal mechanical properties and stability, the pieces were post-cured through exposure to 365 nm UV light for 60 min, rotating every 15 min. A directed heated blower heated the parts to a temperature of about 37 °C during curing.

Bioreactor Loading Regime

Within the bioreactor loading regime set-up, two important inputs should be noted: (1) 1/8 microstepping was used to reduce disjointed motion noise and increase step accuracy and resolution. (2) To reduce heat build-up of the linear actuator over the running time, the hold current during the 12-h rest period was decreased to 0.075 amps/phase rms (run current = 1.5 amps/phase rms) for heat reduction, power savings, and maintenance of the holding position during the wait period.

The intuitive GUI-based IDEA™ software, used to program the bioreactor, provided the ability to modify: speed, distance (i.e., strain), and delay time. The bioreactor program was written to retract a distance corresponding to 12% strain (i.e., 3% unixaxial, cyclic strain applied to scaffolds) at a speed of 0.01 in/s, wait 15 s, extend to the original position at a speed of 0.01 in/s, wait 15 s, and repeat this cycle for 2 h. The wait period was included to allow for the resistance readings to stabilize and to reduce fluctuation and error in resistance readings. After 2 h, the system was held stationary for 12 h before the cycle began again. The bioreactor was run with the repeated cycle for 21 days.

Scaffold Manufacture

The poly-(ε-caprolactone) scaffolds were produced as described in a previous study by Banik et al. where the scaffold design was finalized and analyzed for fiber characteristics, cellular response, and construct mechanics [21]. In brief, the PCL scaffolds were synthesized via electrospinning onto a dual directional rotating rod. Magnets were used to align the fibers along the length of the rod with the oscillating rod tailored fiber alignment. The scaffolds were synthesized as seamless tubes.

Scaffold Bioreactor Positioning

To prepare scaffolds for placement into the bioreactor, 3D-printed t-glase stubs were created to mount the scaffolds. The tendon stubs were designed in Solidworks and processed as STL files in Repetier (an open-access 3D printing software). Prints were completed on a SeeMeCNC Rostock MAX v2 Desktop 3D-printer. Before scaffolds were mounted, the following scaffold dimensions were recorded: mass (Sartorius CP 124S Balance), length (Brown & Sharpe calipers), and diameter (Brown & Sharpe calipers). Scaffold ends were secured by first tightly winding parafilm around the scaffold onto the stubs followed by cinching a zip-tie over the parafilm. It was determined that a notched stub design provided the resistance necessary to prevent the zip-tie from sliding during bioreactor testing; the parafilm acted as a barrier to prevent the zip-tie grip pattern from tearing the scaffold during the mounting process, specifically when tightening the zip-tie.

A measurement tool was created so each scaffold was taut and mounted with equal gauge distances upon placement; this reduced initial error and set the starting point for all scaffolds the same across groups. The gauge length was used to determine the input movement distance or strain percentage.

Cell Seeding and Culture in Bioreactor

All bioreactor mechanical parts were soaked in a series of bleach, distilled water, and 70% ethanol for 20 min each before assembly under the cell culture hood. Mounted scaffolds were submerged in 70% ethanol for 5 min. The scaffolds were allowed to dry overnight under the cell culture hood. Human mesenchymal stem cells, hMSCs, passage 8, purchased from Lonza, Biosciences, were used for dynamic (bioreactor) and static experiments and were applied via micromass seeding with 10,000 cells/cm^2 or about 20,000 cells per scaffold. The cells were distributed on three faces of the scaffold in 67 μL aliquots by allowing the cell/media mixture to penetrate into the scaffold before a new application. The scaffolds were placed in the incubator for 5 min after each application to allow the droplet of cells to soak into the scaffold. This multi-point application method distributed the cells around the scaffold. Cells were not seeded from the inside out.

Grease was applied to the bottom of deep-bottomed polystyrene dishes to prevent the static scaffolds from floating, and dynamic scaffolds were placed into the stub holders of the bioreactor. In both instances, media was filled to cover the

scaffolds completely. The cells were cultured in alpha-modified minimum essential medium (α-MEM, Gibco, Life Technologies), 10% fetal bovine serum (FBS), and 1% penicillin streptomycin (Pen-Strep). Scaffolds were cultured in a standard incubator at 37 °C with 5% CO_2 for 21 days. Media was changed every 3 days.

Histology

Samples from the bioreactor and static groups ($n = 2$) were washed with 1× phosphate-buffered solution (PBS), fixed in 4% paraformaldehyde for 2 h at room temperature and stored in 30% sucrose in 1× PBS overnight. Multiple serial sections were cut with a Leica CM1950 Cryostat at 20 μm slices and stained for Hematoxylin and Eosin (H&E) according to standard procedures (Shandon Gemini Varastainer) to examine the sample structure and composition. Images were acquired using × 10 and × 40 objectives on a fluorescent microscope (Leica DM5500 upright microscope, Leica Microsystems, Buffalo Groove, IL).

Tensile Testing

For tensile testing, the scaffolds were mounted onto custom, 3D-printed stubs to keep the scaffolds in their tubular shape during testing. The stubs were loaded into pressurized grips on an Instron 5960 Dual Column Tabletop tensile machine with a 1 kN load cell and a crosshead speed of 10 mm/min. Time, stress, and strain were output by the software as well as rough estimates of peak stress, initial modulus, and strain-at-breaking; stress was calculated by load/annulus area. Annulus area was measured as mass/(length*density_{PCL}).

Statistical Analysis

Outliers were removed based on the 1.5 interquartile range method. Statistical significance was determined by a one-way ANOVA and a subsequent Tukey's post hoc test with a critical value of $p < 0.05$. The tensile and cellular data presented in this article were obtained through two bioreactor runs.

Results

Bioreactor Design

The 3D-printed bioreactor is composed of three main pieces that work in concert to function as a tendon bioreactor and provide uniaxial, cyclic testing to scaffolds: (1) movement system (i.e., linear actuator/stepper motor, IDEA™

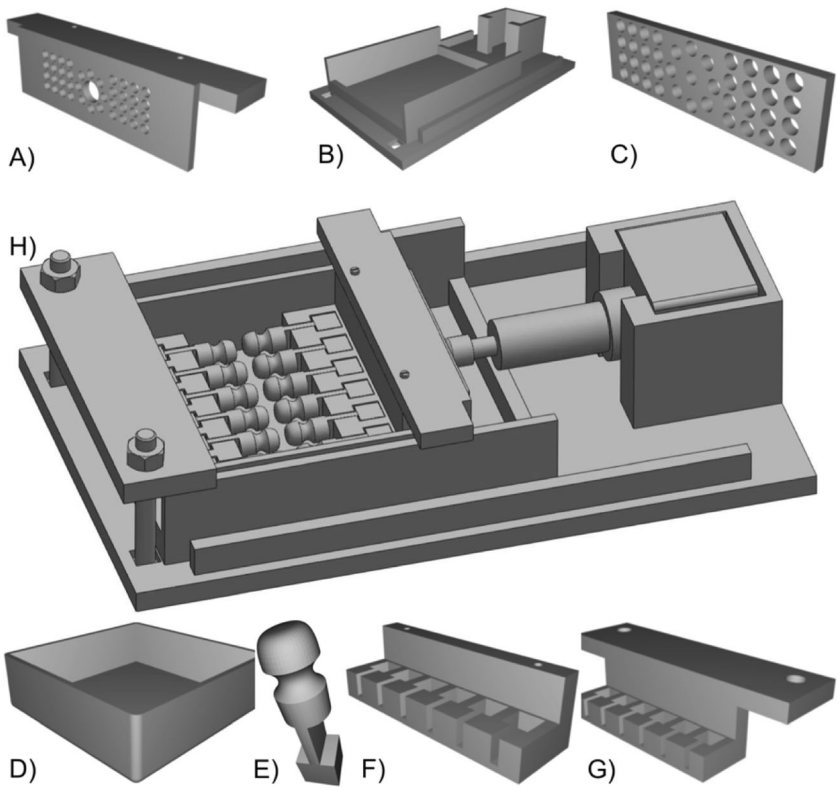

Fig. 1 Graphic reproductions of the Solidworks® pieces designed for the 3D-printed bioreactor pieces. **a** Right-side, attachment to resistance stretch sensor cord. **b** Base. **c** Resistance stretch sensor cord connection between **a** and the nose of the linear actuator. **d** Media and scaffold container. ***e** Scaffold stubs. **f** Right-side stub holder, attaches into **a**. **g** Left-side stub holder mounted to the base. **h** Assembled bioreactor. *Is shown as a representative part but was not 3D-printed

programming drive, and IDEA™ software), (2) conductive rubber cord stretch sensor, and (3) 3D-printed parts and base platform. The Solidworks® representations of the parts are shown in Fig. 1. The individual part files can be found in Supplementary Information.

The bioreactor design is simple and compact with a straightforward approach, as illustrated in Fig. 2. The scaffold container holds up to six scaffolds at once; the single chamber makes changing the media easy and reduces the amount of media required for each media change. Alligator clips connected to the stretch sensor and multimeter relay values that reflect the resistance readings based on the change in length of the stretch sensor cord. The stretch sensor cord is woven through 40 holes to create a rigid system. The Haydon Kerk component trio—linear actuator, stepper motor controller, and programming interface program—comprise the smooth mechanical system which provides the uniaxial, cyclic stretch. Another benefit to this combination is that the only mechanical component that must be able to withstand the humidity and heat from the incubator is the linear actuator. The controller was connected such that it can be placed outside the incubator along with the power source and multimeter. This is an inherent benefit because it prolongs life of the mechanical components and reduces concerns related to housing electrical components and connectors in a humidified environment.

The lack of multiple screws and components with cracks and crevices lessened the chances for contamination and bacteria. The straightforward design simplifies troubleshooting issues and makes replacing parts as easy as pushing a printer button. Bioreactor build time is less than 10 min after parts are 3D-printed, sterilized, and the resistance cord is woven and secured.

Bioreactor System Validation

The bioreactor was verified for functionality by investigating input and output correlations. The time required for the resistance readings to have minimal fluctuations (i.e., delay time between loading and unloading when a force is applied or removed) were analyzed in order to understand the general time it took for the resistance stretch cord to return to its original length; the time required was established to be about 15 s. Validation tests were also performed to understand the characteristics and responses from the stretch sensor and determine the input and output resistance readings based on the distance the scaffold was moved. It can be noted in Fig. 3a, where strains lower than 6% are presented, that the initial return resistance was consistent across each retraction and as the strain percentage was increased a noticeable increase of resistance readings reflected this change. The graph in Fig. 3b

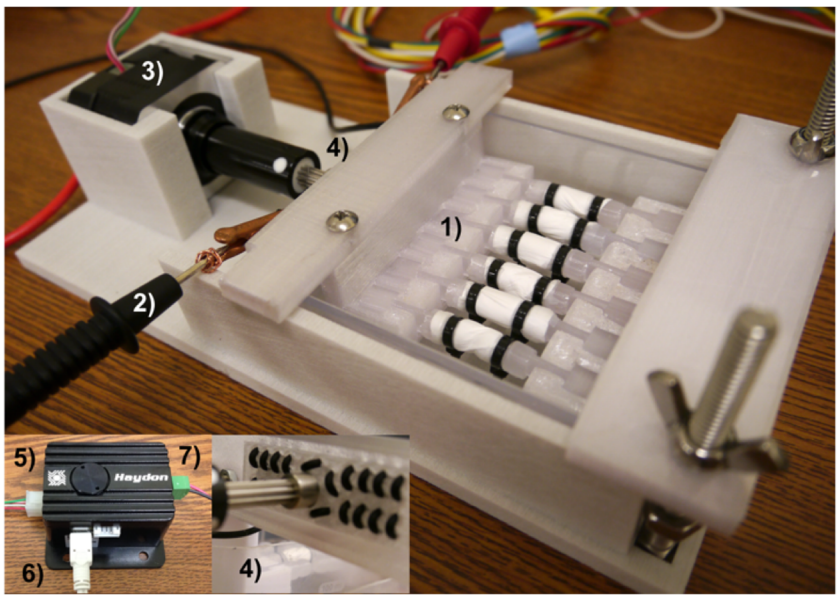

Fig. 2 The final bioreactor version has the ability to house up to 6 scaffolds (1). The framework and individual parts were 3D-printed, which lends the bioreactor to being widely accessible, cost effective, flexible in design, and reproducible. The real-time resistance readout is completed through a construction of a stretch sensor cord (2, 4) to allow for correlations to stress or strain. To drive the cyclic strain system, an IDEA™ programmable stepper motor controller (5) (located outside of the incubator) was used to power a programmable linear actuator (3) (located in the incubator) (Haydon Kerk). An additional benefit of the presented bioreactor is that a consistent computer connection is not required. Within the IDEA™ controller interface program, a start program can be designated to automatically begin upon supply of power rather than relying on pulling from a program embedded in a computer interface package. Once the program is uploaded to the IDEA™ controller as the "start program," connection 6 can be removed. Connection point 7 provides the connection to a voltage source for power

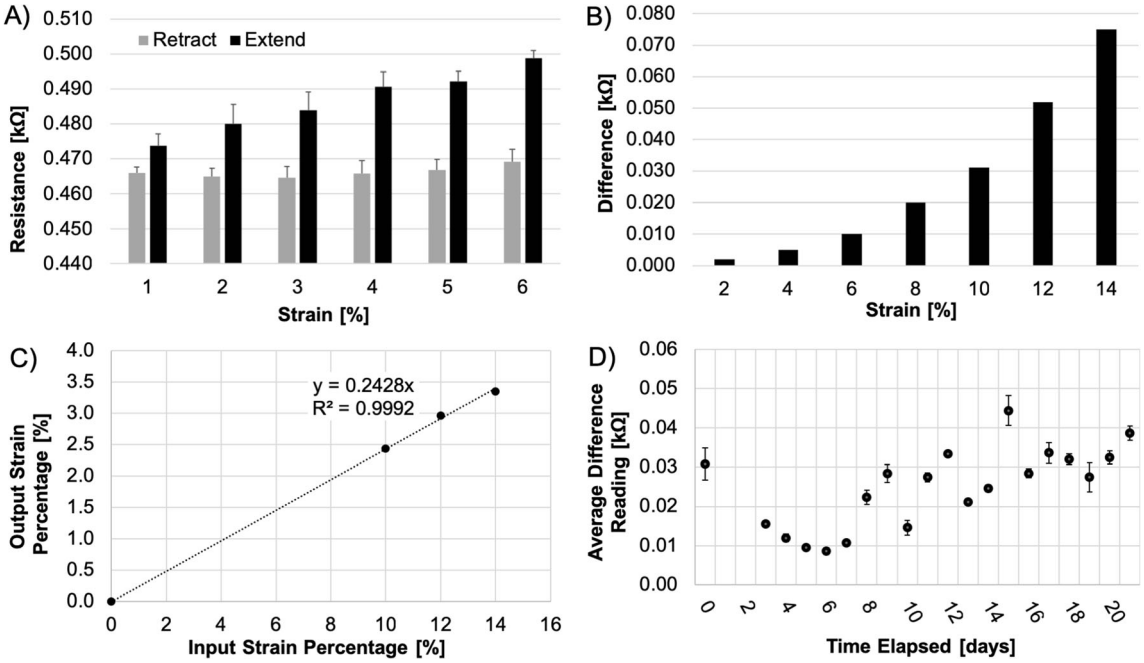

Fig. 3 **a**, **b** Bioreactor validation tests were performed to understand the relationship between a change in length of the stretch sensor cord (i.e., strain) vs. the output resistance readings. Each group was significantly different from all other groups by $p < 0.001$ in the top graph. **c** With six scaffolds loaded in the bioreactor, it was determined that there was a linear correlation between the input strain and output strain. This relationship was used to more accurately apply the intended strain to the scaffolds during testing. **d** The constructed bioreactor was utilized to apply 3% uniaxial, cyclic strain to the scaffolds for 2 h with a 12-h rest period for 21 days. Ten resistance readings were manually read from the multimeter and recorded every other active period. The resistance differences were determined between the consecutive high and low values, averaged for each day, and plotted to show the trend in scaffold response over time. (Resistance differences, $n = 5$, for each reading)

shows larger strain percentages ranging from 2 to 14% and demonstrates the relationship between the change in length of the stretch sensor cord and the difference in resistance readings to the retraction and extension motions.

A linear correlation ($y = 0.2428x$) with an R^2 value of 0.9992 was determined when the input strain percentage versus output strain percentage was compared (Fig. 3c). The input strain was the value entered into the program based on the gauge length of the scaffolds. The output strain was measured using ImageJ. Due to the small length changes for the lower strain percentages, higher input strain percentages, 12–14%, were used in order to improve the accuracy of the measurements in ImageJ.

Bioreactor Resistance Readings

The bioreactor was actively running for 2 h at 3% strain applied to the scaffolds before it entered a 12-h rest period; this cycle was repeated for 21 days. Ten resistance readings (i.e., five retraction and five extension readings) were recorded manually every other active period. The resistance differences of the high and low readings were calculated, and the averages of these five values were recorded and plotted with standard deviations for each of the 12–16 h value readouts (Fig. 3d).

The results from the 21 days of readings show an overall trend towards an increase in resistance readings by the end of the culture period. A dip in resistance reading differences was noted for the first 7 days followed by an increase for 3 days before the readings begin fluctuating for the next 9 days. The last 3 days of culture time reflect an increase in resistance readings.

Cell Response to Cyclic, Dynamic Culture in the Bioreactor

H&E staining was used to identify ECM and collagen production throughout the scaffolds. By using fluorescence microscopy, the Eosin stain was highlighted such that the collagen structure and content was emphasized. The H&E image demonstrates a prospective increase in cell proliferation over time. Fluorescent images of Eosin staining at × 10 and × 40 magnification are shown in Fig. 4. While the collagen fiber arrangement has no discernible pattern, collagen and ECM production is definitively more apparent throughout the dynamic sample. The staining suggests the presence of cells due to the high ECM and collagen content. Imaging the H&E slides with normal brightfield microscopy yielded colors too faint to image; thus, fluorescent microscopy was revealed to be a better technique for illustrating the elastin and collagen content.

Tensile testing was performed, $n = 5$, on the scaffolds seeded in the bioreactor for 21 days and cell-free scaffolds, $n = 6$ (Fig. 5). The elastic moduli result of dynamic bioreactor culturing was impressive with about a × 10 fold increase

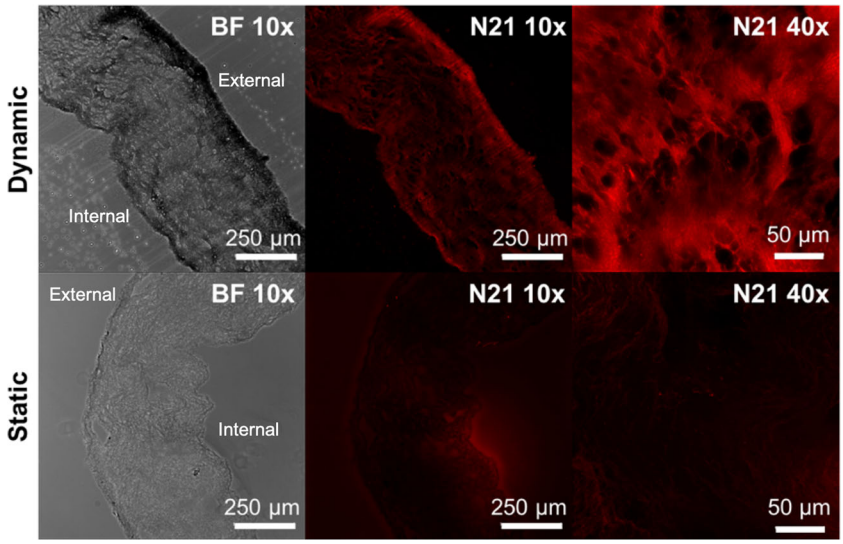

Fig. 4 Dynamic (application of 3% uniaxial, cyclic strain for 2 h with a 12-h rest period for 21 days) and static (cultured in TCPS dishes for 21 days) samples were fixed and processed for histology. Samples were stained with H&E staining and imaged with fluorescence microscopy (N2.1 filter cube) to fluoresce the Eosin staining and better image the elastic and collagen fibers in the samples. ($n = 1$, exposure times were kept consistent in groups of brightfield and N21 and × 10 and × 40)

compared to scaffolds without cells. Static scaffolds without cells exhibited 30.33 ± 8.37 MPa elastic moduli while the dynamic scaffolds cultured with cells in the bioreactor presented an average elastic moduli of 216.53 ± 55.71 MPa. The cell-free scaffold controls from previous tests demonstrated an average value of 36.5 ± 9.0 MPa for 184 rpm scaffolds, 24.4 ± 6.6 MPa for 216 rpm scaffolds, 30.3 ± 8.4 MPa for 264 rpm scaffolds, and 30.7 ± 5.0 MPa for 328 rpm scaffolds [21]. The toe region values were 0.49 ± 0.43% and 3.35 ± 1.12% for the static cell-free scaffolds and cell-seeded scaffolds, respectively. The toe region upper boundaries for the cell-free scaffold controls were as follows: for 184 rpm, 5.3 ± 2.8%, for 216 rpm, 6.7 ± 3.0%, for 264 rpm, 3.4 ± 1.1%, and for 328 rpm, 0.5 ± 0.7%.[21] The differences shown between the two scaffold groups were significant to the level of $p < 0.001$.

Discussion

A bioreactor system was used to create an environment to better mimic in vivo loading conditions compared to static culture [22]. The utilization of a bioreactor allows for testing to be conducted in a controlled, closed system

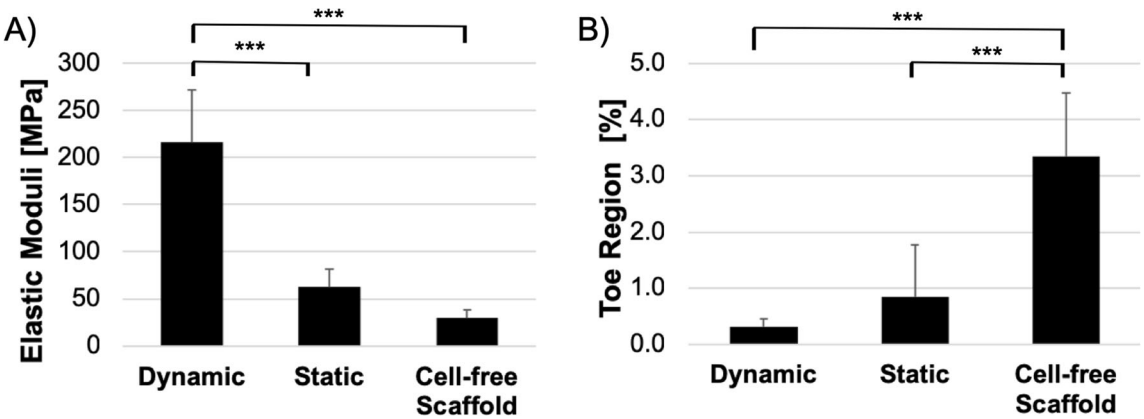

Fig. 5 Samples were mechanically tested to investigate the effects of cells and the application of cyclic strain on the elastic moduli and toe region. The "Dynamic" group was represented by scaffolds seeded with 20,000 cells per scaffold and cultured in the bioreactor for 21 days with application of 3% uniaxial, cyclic strain for 2 h with a 12-h rest period in between each active period. The "Static" group were electrospun scaffolds seeded with 20,000 cells per scaffold and cultured in a petri dish for 21 days without any applied strain. The "PCL Scaffold" group were electrospun scaffolds composed of polycaprolactone (PCL) without cells and without cyclic strain. (elastic moduli: $n = 5$, dynamic and static, $n = 6$, PCL scaffold, toe region: $n = 5$, dynamic, static, and cell-free scaffold; outliers were removed by the 1.5 interquartile range test; * $p < 0.05$; ** $p < 0.01$; *** $p < 0.001$)

where mechanical stimulation can be added while concurrently monitoring the biological processes influenced by the mechanical means [23]. The principle behind the system is that cells can receive signals from their surrounding environment and will respond to the chemical, mechanical, and physical stimuli through directed cell growth and behavior, such as alignment and differentiation. Static culture has been demonstrated to be poor in stimulating positive cell growth and has often resulted in lower seeded constructs with necrotic cells in the center of the scaffold [7]. Therefore, it was anticipated that the bioreactor system would promote heterogeneous cell distribution with sufficient mass and nutrient transfer in the system.

It has been stated that DNA content and protein synthesis in human tenocytes increase with repetitive motion, such as those that can be simulated with a bioreactor [24]. A key function of tendons is force transmission, and, therefore, tendons inherently benefit from mechanical stimulation, such as uniaxial strain, for scaffold maintenance and mechanics, gene expression, and cell development and differentiation when conditioned in a bioreactor [22, 25, 26]. Previous research has demonstrated increases in ultimate tensile strength and elastic moduli values following mechanical treatment in a bioreactor [27].

The idea to introduce 3D printing into the design for reduced cost and increased design flexibility was a large influence in the direction of the bioreactor. All mechanisms are positioned in a linear, parallel fashion to eliminate the potential for torque to occur between components. The smaller bioreactor components were printed via SLA-printing to prevent accumulation of media as the parts were immersed in the media.

The design flexibility of the bioreactor makes it such that it can be revised to meet the needs of different research groups. Using 3D printing to build the bioreactor allows for multiple iterations of parts and designs to be tested and constructed quickly and inexpensively. The 3D-printed design of the bioreactor also increases accessibility to this technology. The design met the goal to create a low-cost device, with the total cost under $750. The validation tests were valuable to understand the resistance stretch sensor cord responses to a change in length as well as how sensitive the readout values would be (Fig. 3a, b) and the appropriate inputs in terms of the expected applied strain to the scaffolds (Fig. 3c). Without these relationships, it would have been difficult to ensure effective device function.

Mechanical loading to the cell-seeded constructs elicited exciting responses to the applied cyclic strain, specifically in relation to the mechanical output based on the recorded resistance readings and elastic moduli. The graph in Fig. 3d suggests that the scaffolds were indeed positively changing in mechanics over the 21-day time period in culture. Due to the nature of the variability in the resistance cord set-up (i.e., tautness of the cord), the recorded resistance value differences (Fig. 3d) do not mean anything numerically relative to the scaffold strength. The qualitative analysis of the trend is the only data that remains valuable in understanding the scaffold's response and changes over time. Variability between the recorded retraction and extension values is little to none, which suggests that the program is effective in ensuring an appropriate delay time between each active period. The minor standard deviations also suggest validation in the accuracy of the motor components to relay the appropriate movement length.

The increases in ECM/collagen content and mechanics (Figs. 4 and 5) provide promise for the proposed scaffold and bioreactor design in tendon tissue engineering applications and future research. A number of research groups have used fluorescent imaging of H&E staining to better display certain features in the histological section with benefits such as displays proximal and distal differences [28], intensifies inconspicuous components like elastin [29], and requires no extra sample processing [30]. Deeb et al. showed that the sensitivity of using fluorescence microscopy on H&E samples can reveal localized elastic fibers and collagen and could be considered as an equivalent to Weigert's or Masson's trichrome stains when looking at these tissue components [31]. This technique was applied to the bioreactor sections due to the difficulty to see the colors and morphology with brightfield light microscopy. It is anticipated that the mechanical loading applied by the uniaxial, cyclic strain bioreactor increases cell polarization and reorients actin stress fibers to ultimately increase the scaffold mechanics and appropriate ECM and collagen production.

Bioreactors are crucial in tissue engineering research for product and tissue development, standardizing tissue manufacturing procedures, quality control, and large-scale synthesis. While previous research has demonstrated the importance of mechanical loading for tendon healing, the relationships between a specific strain, frequency, and duration, and the tenogenic response is currently still not well understood [5]. The results from the bioreactor conditioning of the scaffolds not only lends to a better understanding of how specific inputs affect the tissue outcomes but also demonstrates the capability of the presented hobbyist grade, 3D-printed bioreactor. The accessibility of the bioreactor is a significant development for researchers to conduct in-house dynamic in vitro testing to advance their research in a more physiological and applicable method. Furthermore, the flexibility provided in the 3D-printed bioreactor design enables simple modifications to accommodate a range of possible tissue-engineered constructs.

Conclusions

A bioreactor was constructed with the following criteria established: real-time readout of resistance, ability to be easily cleaned and sterilized, control of strain, speed, and time parameters, and capability to withstand 3 weeks of continuous load with minimal maintenance. The scaffolds cultured in a dynamic setting showed improved mechanics and promising ECM and collagen content generated. The presented bioreactor is simple in design and construction and provides the effective cyclic stretch and physiological, dynamic conditions necessary for improving cellular commitment and tissue growth specific to tendon tissue. Future work includes conducting experimental repeats, additional cellular response characterization, and integrating a Graphic User Interface (GUI) for the bioreactor.

Acknowledgments Gene Gerber, Tony Banik, Andrew Higgins, Jordan Dover, Gary Meyers, Austin Greever, Greg Learn, Eric VanArsdale, Michele Herneisey, and Nimesh Lad are acknowledged for their input on the bioreactor design and iterations. John Cantolina is recognized for his help with histology.

Funding Information This material was based upon work supported by R03 AR065192 and the National Science Foundation (NSF) under Grant No. DGE1255832. Any opinions, findings, and conclusions or recommendations expressed in this material are those of the authors and do not necessarily reflect the views of the NSF.

Compliance with Ethical Standards

Conflict of Interest The authors declare that they have no conflict of interest.

References

1. Youngstrom DW, Barrett JG. Engineering tendon: scaffolds, bioreactors, and models of regeneration. Stem Cells Int. 2016;2015:1–11.
2. Matheson LA, Fairbank NJ, Maksym GN, Santerre JP, Labow RS. Characterization of the Flexcell (TM) Uniflex (TM) cyclic strain culture system with U937 macrophage-like cells. Biomaterials. 2006;27:226–33.
3. Youngstrom DW, Rajpar I, Kaplan DL, Barrett JG. A bioreactor system for in vitro tendon differentiation and tendon tissue engineering. Andarawis-Puri N, Flatow EL, Soslowsky LJ, editors. J Orthop Res. 2015;33:911–8.
4. Wang T, Lin Z, Day RE, Gardiner B, Landao-Bassonga E, Rubenson J, et al. Programmable mechanical stimulation influences tendon homeostasis in a bioreactor system. Biotechnol Bioeng. 2013;110:1495–507.
5. Wang T, Lin Z, Ni M, Thien C, Day RE, Gardiner B, et al. Cyclic mechanical stimulation rescues achilles tendon from degeneration in a bioreactor system. J Orthop Res. 2015;33:1888–96.
6. Maeda E, Hagiwara Y, Wang JH-C, Ohashi T. A new experimental system for simultaneous application of cyclic tensile strain and fluid shear stress to tenocytes in vitro. Biomed Microdevices. 2013;15:1067–75.
7. Plunkett N, O'Brien FJ. Bioreactors in tissue engineering. Technol Health Care. 2011;19:55–69.
8. Zhao J, Griffin M, Cai J, Li S, Butler P, Kalaskar DM. Bioreactors for tissue engineering: an update. Biochem Eng J. 2016;109:268–81.
9. Eyckmans J, Boudou T, Yu X, Chen CS. A hitchhiker's guide to mechanobiology. Dev Cell. 2011;21:35–47.
10. Chaturvedi LS, Marsh HM, Basson MD. Src and focal adhesion kinase mediate mechanical strain-induced proliferation and ERK1/2 phosphorylation in human H441 pulmonary epithelial cells. Am J Physiol Cell Physiol. 2007;292:C1701–13.
11. Driscoll TP, Cosgrove BD, Heo S-J, Shurden ZE, Mauck RL. Cytoskeletal to nuclear strain transfer regulates YAP signaling in mesenchymal stem cells. Biophys J. 2015;108:2783–93.
12. Boutahar N, Guignandon A, Vico L, Lafage-Proust M. Mechanical strain on osteoblasts activates autophosphorylation of focal adhesion kinase and proline-rich tyrosine kinase 2 tyrosine sites involved in ERK activation. J Biol Chem. 2004;279:30588–99.
13. Hong S-Y, Jeon Y-M, Lee H-J, Kim J-G, Baek J-A, Lee J-C. Activation of RhoA and FAK induces ERK-mediated osteopontin expression in mechanical force-subjected periodontal ligament fibroblasts. Mol Cell Biochem. 2010;335:263–72.
14. Guilak F, Cohen DM, Estes BT, Gimble JM, Liedtke W, Chen CS. Control of stem cell fate by physical interactions with the extracellular matrix. Cell Stem Cell. 2009;5:17–26.
15. Higgins AM, Banik BL, Brown JL. Geometry sensing through POR1 regulates Rac1 activity controlling early osteoblast differentiation in response to nanofiber diameter. Integr Biol. 2015;7:229–36.
16. Ozdemir T, Xu L-C, Siedlecki C, Brown JL. Substrate curvature sensing through Myosin IIa upregulates early osteogenesis. Integr Biol. 2013;5:1407–16.
17. Gao L, McBeath R, Chen CS. Stem cell shape regulates a chondrogenic versus myogenic fate through Rac1 and N-cadherin. Stem Cells. 2010;28:564–72.
18. Kim H, Sonn JK. Rac1 promotes chondrogenesis by regulating STAT3 signaling pathway. Cell Biol Int. 2016;40:976–83.
19. Woods A, Beier F. RhoA/ROCK signaling regulates chondrogenesis in a context-dependent manner. J Biol Chem. 2006;281:13134–40.
20. McBeath R, Fertala A, Risbud M, Shapiro I, Osterman L. Hypoxia drives tenocyte differentiation. J Hand Surg. 2013;38:e11.
21. Banik BL, Lewis GS, Brown JL. Multiscale poly-(ϵ-caprolactone) scaffold mimicking non-linearity in tendon tissue mechanics. Regen Eng Transl Med. 2016;2:1–9.
22. Wang T, Gardiner BS, Lin Z, Rubenson J, Kirk TB, Wang A, et al. Bioreactor design for tendon/ligament engineering. Tissue Eng B. 2012;19:133–46.
23. Martin I, Wendt D, Heberer M. The role of bioreactors in tissue engineering. Trends Biotechnol. 22:80–6.
24. Sharma P, Maffulli N. Tendon injury and tendinopathy: healing and repair. J Bone Joint Surg. 2005;87:187–202.
25. Nirmalanandhan VS, Dressler MR, Shearn JT, Juncosa-Melvin N, Rao M, Gooch C, et al. Mechanical stimulation of tissue engineered tendon constructs: effect of scaffold materials. J Biomech Eng. 2007;129:919–23.
26. Angelidis IK, Thorfinn J, Connolly ID, Lindsey D, Pham HM, Chang J. Tissue engineering of flexor tendons: the effect of a tissue bioreactor on adipoderived stem cell–seeded and fibroblast-seeded tendon constructs. J Hand Surg. 2010;35A:1466–72.
27. Saber S, Zhang AY, Ki SH, Lindsey DP, Smith RL, Riboh J, et al. Flexor tendon tissue engineering: bioreactor cyclic strain increases construct strength. Tissue Eng A. 2010;16:2085–90.
28. McMahon JT, Myles JL, Tubbs RR. Demonstration of immune complex deposits using fluorescence microscopy of hematoxylin

and eosin–stained sections of Hollande's fixed renal biopsies. Mod Pathol. 2002;15:988–97.
29. Heo YS, Song HJ. Characterizing cutaneous elastic fibers by eosin fluorescence detected by fluorescence microscopy. Ann Dermatol. 2011;23:44–52.
30. Elston DM. Medical Pearl: Fluorescence microscopy of hematoxylin-eosin-stained sections. J Am Acad Dermatol. 2002;47:777–9.
31. Deeb S, Nesr KH, Mahdy E, Badawey M, Badei M. Autofluorescence of routinely hematoxylin and eosinstained sections without exogenous markers. Afr J Biotechnol. 7:504–7.